Topological Network Analysis of Electroencephalographic Power Maps

Yuan Wang(✉), Moo K. Chung, Daniela Dentico, Antoine Lutz, and Richard J. Davidson

University of Wisconsin, Madison, USA
yuanw@stat.wisc.edu

Abstract. Meditation practice is a non-pharmacological intervention that provides both physical and mental benefits. It has generated much neuroscientific interest in its effects on brain activity. Spontaneous brain activity can be measured by electroencephalography (EEG). Spectral powers of EEG signals are routinely mapped on a topographic layout of channels to visualize spatial variations within a certain frequency range. In this paper, we propose a *node-based network filtration* to model the spatial distribution of an EEG topographic power map via its dynamic local connectivity with respect to a changing scale. We compare topological features of the network filtrations between long-term meditators and mediation-naïve practitioners to investigate if long-term meditation practice changes power patterns in the brain.

1 Introduction

Meditation is a set of mental training regimes widely practiced for its claimed benefits to physical and mental health. The investigation of spontaneous brain activity during resting state or practice, is a sensitive approach to identify neuroplastic changes induced by meditation practice [2]. Electroencephalogram (EEG) is an important imaging modality for exploring the neuroplastic effects of meditation under various experimental conditions. In these studies, spectral powers of EEG signals are routinely mapped on a topographic layout of channels to visualize spatial variations within a certain frequency range. Topographic difference in spectral powers indicates configuration change in the brain's active neuronal sources. It is thus important to establish a statistical framework for comparing topographic power maps in the study of neuroplastic effect of long-term meditation practice.

Statistical inference of EEG topographic power maps is typically based on the mass univariate approach with multiple node-level testing [7]. This approach does not account for the network topology in the topography of the power map. Alternative statistical methods more commonly applied to electric potential maps include microstate analysis [1] and cluster-based inference [8]. But microstate analysis uses a global dissimilarity index based on node-level mean

G. Wu et al. (Eds.): CNI 2017, LNCS 10511, pp. 134–142, 2017.
DOI: 10.1007/978-3-319-67159-8_16

difference and variance rather than network topology in the topography. Cluster-based methods often require threshold selection which may result in bias and inconsistency [5,9].

In this paper, we propose a *node-based network filtration* for modeling the spatial distribution of an EEG topographic power map. Each EEG power map is modeled as an undirected network on a triangulation of the map, with node weights defined from denoised frequency powers. We binarize the network by thresholding the node weights, and obtain the network filtration - a nested sequence of binary networks - as we vary the threshold. A topological feature of the filtration is then incorporated in a permutation test for group difference between the maps. Simulation studies show evidence that the proposed framework is robust to scaling and translation of maps and sensitive to translation in opposite directions resulting in map spatial difference. The proposed framework is also applied to compare the topographic power maps of long-term meditators and meditation naïve practitioners.

The methodological contributions of this paper are: (1) we propose a node-based network filtration for quantifying the spatial distribution of an EEG topographic power map; (2) we use the node-based network filtration to make spatial comparison of two groups of EEG power maps.

2 Methods

Our goal is to compare spatial distribution of EEG power maps in meditators and novices. We first briefly describe a spatial denoising procedure on a power map. We then characterize the spatial distribution of the denoised power map through a sequence of binary networks constructed on the map.

EEG topographic power map. Signal at each of the c observed EEG channels $v_1, v_2, \ldots, v_c$ is decomposed into frequency components by Fourier transform. The strengths of the frequency components within a certain range are measured by integrating the power spectral density (PSD). Here we estimate the PSD of the EEG signal at each channel by Welch's method of modified periodogram: divide a signal into overlapping segments and then average the modified periodograms computed on all the segments to obtain a PSD estimate with reduced variance than the usual periodogram [10]. We denote the topographic map of the PSDs at c EEG channels by $\boldsymbol{f} = (f_1, \ldots, f_c)$, where the index follows the EEG channel labels.

Spatial denoising. We then spatially denoise the topographic power map $\boldsymbol{f}$ of each subject at a particular frequency band. We model the topography of $\boldsymbol{f}$ as an undirected graph $\mathcal{G} = \{\mathcal{V}, \mathcal{E}\}$ with the node set

$$\mathcal{V} = \{v_i : i = 1, \ldots, c\}$$

of the c EEG channels and the edge set with no orientation

$$\mathcal{E} = \{(v_i, v_j) : v_i, v_j \in \mathcal{T}_{\mathcal{V}}, v_i \sim v_j, i, j = 1, \ldots, c\},$$

where $\mathcal{T}_{\mathcal{V}}$ is the Delaunay triangulation built on $\mathcal{V}$ and $\sim$ denotes neighbors in $\mathcal{T}_{\mathcal{V}}$. Defining the graph Laplacian $L = (l_{ij})$ on $\mathcal{G}$ by

$$l_{ij} = \begin{cases} -a_{ij}, & v_i \neq v_j \text{ and } v_i \sim v_j \\ \sum_{k \neq i} a_{ik}, & v_i = v_j \\ 0, & \text{otherwise} \end{cases}$$

with the adjacency matrix $A = (a_{ij})$, there are up to c unique eigenvectors $\psi_1, \psi_2, \cdots, \psi_c$ satisfying

$$L\psi_j = \gamma_j \psi_j \tag{1}$$

with $0 \leq \gamma_1 \leq \gamma_2 \leq \cdots \leq \gamma_c$. These eigenvectors are orthonormal, i.e., $\psi_i' \psi_j = \delta_{ij}$ - the Kronecker's delta. The first eigenvector is trivial: $\psi_1 = 1/\sqrt{c}(1, \ldots, 1)'$. All other eigenvalues and eigenvectors are analytically unknown and need to be numerically computed.

Once we obtain eigenvectors ψ_j satisfying (1) on the Delaunay triangulation $\mathcal{T}_{\mathcal{V}}$, the heat kernel estimate for the power map $\boldsymbol{f}$ is given by

$$\widehat{\boldsymbol{f}} = (\widehat{f}_1, \ldots, \widehat{f}_c) = K_\sigma * \boldsymbol{f} = \sum_{j=1}^{c} e^{-\gamma_j \sigma} \zeta_j \psi_j, \tag{2}$$

where $K_\sigma = \sum_{j=1}^{c} e^{-\gamma_j \sigma} \psi_j \psi_j'$ is the discrete heat kernel and $\zeta_j = \boldsymbol{f}' \psi_j = \psi_j' \boldsymbol{f}, j = 1, \ldots, c$, are the Fourier coefficients with respect to the basis $\{\psi_1, \ldots, \psi_c\}$. The parameter σ is the heat kernel bandwidth and it modulates the extent of denoising.

Quantifying the spatial distribution of a power map. We define a node-weighted network on the map through $\mathcal{G} = \{\mathcal{V}, \mathcal{E}\}$, with the node weights

$$w_i = \widehat{f}_i, i = 1, \ldots, c,$$

assumed to be unique. With respect to an arbitrary threshold $\lambda \in \mathbb{R}$, we define a binary network

$$\mathcal{G}_\lambda = \{\mathcal{V}_\lambda, \mathcal{E}_\lambda\}$$

on $\mathcal{G}$, where

$$\mathcal{V}_\lambda = \{v_i \in \mathcal{V} : w_i \leq \lambda\}$$

and

$$\mathcal{E}_\lambda = \{(v_i, v_j) \in \mathcal{E} : \max(w_i, w_j) \leq \lambda\}.$$

Now let

$$\lambda_1 = w_{(1)} < \lambda_2 = w_{(2)} < \cdots < \lambda_c = w_{(c)}$$

be the order statistics of the unique node weights $w_1, w_2, \ldots, w_c$ of $\mathcal{G}$. Setting λ in the order of $\lambda_1, \lambda_2, \cdots, \lambda_c$ yields a sequence of subsets of $\mathcal{G}$:

$$\mathcal{G}_{\lambda_1} \subset \mathcal{G}_{\lambda_2} \subset \cdots \subset \mathcal{G}_{\lambda_c}, \tag{3}$$

which we call a *node-based network filtration*.

Note that the filtration (3) is not affected by relabeling of the EEG channels, since the order statistics $\lambda_i = w_{(i)}, i = 1, \ldots, c$, remain the same regardless of the channel labels. Each $\mathcal{G}_\lambda$ in (3) consists of clusters of nodes; as λ increases, clusters appear and later merge with existing clusters. The pattern of changing clusters in (3) has the following key properties.

(1) For all $\lambda_i < \lambda < \lambda_{i+1}$, $\mathcal{G}_\lambda = \mathcal{G}_{\lambda_i}, i = 1, \ldots, c-1$; in other words, the filtration (3) is maximal in the sense that no more $\mathcal{G}_\lambda$ can be added to it.

(2) As λ increases from λ_i to λ_{i+1}, only the node v'_{i+1} that corresponds to the weight λ_{i+1} is added in $\mathcal{V}_{\lambda_{i+1}}$.

(3) Define a local minimum (maximum) λ_i as

$$\lambda_i < \lambda_j \ (\lambda_i > \lambda_j), \forall\ v'_j \sim v'_i,$$

where v'_i and v'_j are nodes that correspond to the weights λ_i and λ_j. New cluster of nodes emerge in $\mathcal{G}_{\lambda_i}$ at a local minimum λ_i and merge with other clusters at a local maximum λ_i. Here we assume that we do not encounter the case where

$$\lambda_i < \lambda_j \text{ some } v'_j \sim v'_i \text{ and } \lambda_i > \lambda_j \text{ the other } v'_j \sim v'_i.$$

Properties (1) and (2) hold because the $\lambda_i, i = 1, \ldots, c$ account for all the unique node weights $w_i, i = 1, \ldots, c$. Property (3) holds for local minimum λ_i because all the neighboring nodes v'_j of v'_i are not included in $\mathcal{G}_{\lambda_i}$, hence v'_i emerges as a standalone cluster in $\mathcal{G}_{\lambda_i}$; for local maximum λ_i, clusters to which the v'_j are connected are joined by v'_i in $\mathcal{G}_{\lambda_i}$.

We illustrate the filtration (3) on a 6-channel EEG layout in the international 10–20 system (Fig. 1). We first build up the Delaunay triangulation over the 6-channel layout (Fig. 1). Node weights are the powers at the EEG channels. At each filtration value λ, we include the nodes and edges with weights less than or equal to λ. The clusters change as λ increases.

Topological permutation test. We use a topological feature to summarize the changing connectivity in the sequence of binary networks. The 0th Betti number β_0 counts the number of clusters in a network [4]. In this paper we define the 0th Betti function at $\lambda_1 < \cdots < \lambda_m$ as the sequence of 0th Betti numbers $(\beta_0^1, \ldots, \beta_0^m)$. For instance, the 0th Betti function in Fig. 1 corresponding to $\lambda = -1, 0, 0.5, 1, 2, 3$ is (1, 1, 2, 1, 1, 1).

Same spatial distribution implies the same node-based network filtration, hence the same 0th Betti function. To statistically compare the spatial distribution of two groups of denoised power maps, we test the null hypothesis that there is no difference between the respective mean 0th Betti functions $\bar{\beta}_0^1$ and $\bar{\beta}_0^2$ of the node-based network filtrations of maps in Group 1 and 2:

$$H_0 : \bar{\beta}_0^1(\lambda) = \bar{\beta}_0^2(\lambda), H_1 : \bar{\beta}_0^1(\lambda) \neq \bar{\beta}_0^2(\lambda), \tag{4}$$

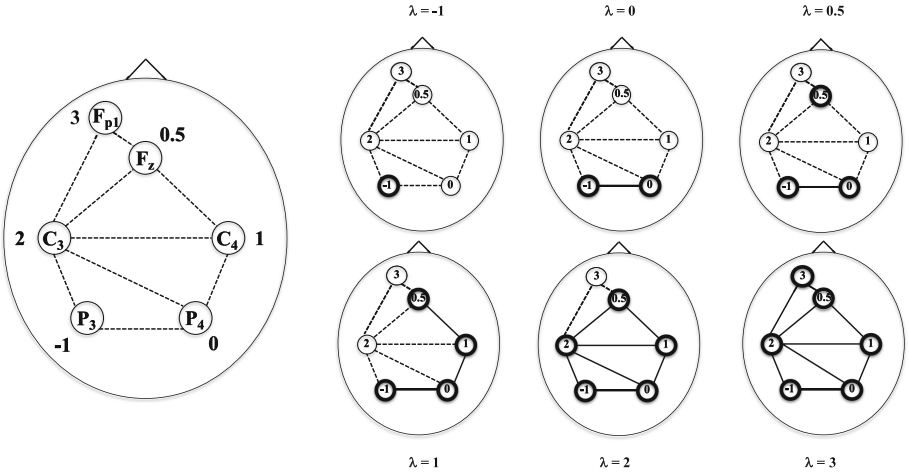

Fig. 1. Schematic of the filtration (3) on 6 weighted EEG channels in the international 10–20 system. (a) Large figure on left: The 6-channel layout with the corresponding Delaunay triangulation indicated by dashed lines. Node weights are the powers at the EEG channels. (b) Small figures on right: At each filtration value λ, we include the nodes and edges with weights less than or equal to λ. As the λ increases, more nodes and edges join in the filtration.

at fixed m filtration values $\lambda_1, \ldots, \lambda_m$. To test the null hypothesis (4), we first compute the ℓ_2 distance

$$\ell_2(\bar{\beta}_0^1, \bar{\beta}_0^2) = \sqrt{\sum_{i=1}^{m} (\bar{\beta}_0^1(\lambda_i) - \bar{\beta}_0^2(\lambda_i))^2}, \tag{5}$$

between the respective group means

$$\bar{\beta}_0^1 = (\bar{\beta}_0^1(\lambda_1), \ldots, \bar{\beta}_0^1(\lambda_m)) \text{ and } \bar{\beta}_0^2 = (\bar{\beta}_0^2(\lambda_1), \ldots, \bar{\beta}_0^2(\lambda_m))$$

of the 0th Betti functions of the node-based network filtrations characterizing the denoised power maps in Group 1 and 2. Then the labels of the two groups undergo repeated random exchanges. At each label exchange, the $\ell_2(\bar{\beta}_0^{1'}, \bar{\beta}_0^{2'})$ distance between the respective mean Betti functions $\bar{\beta}_0^{1'}$ and $\bar{\beta}_0^{2'}$ of the relabeled power maps. We take the proportion of the distances $\ell_2(\bar{\beta}_0^{1'}, \bar{\beta}_0^{2'})$ exceeding that of the observed distance $\ell_2(\bar{\beta}_0^1, \bar{\beta}_0^2)$ is taken as the p-value for the permutation test.

3 Simulations

We use simulations to evaluate how well the proposed topological permutation test detects difference in the spatial distribution of two groups of power maps.

A scaled or translated map has identical filtration as the original map after normalization. So the proposed test should stay robust under map scaling and translation with moderate noisy perturbations. It should also be sensitive to spatial difference between maps caused by translation in opposite directions.

We simulate two groups of noisy power maps by first defining the underlying function $\boldsymbol{z} = (z_1, \ldots, z_{100})$ by

$$z_i = 3(1 - x_i)^2 e^{-(x_i^2 + y_i^2)} + 3e^{-((x_i - 2)^2 + y_i^2)}, i = 1, \ldots, 100, \tag{6}$$

with the Cartesian coordinates $(x_1, y_1), \ldots, (x_{100}, y_{100})$ sampled uniformly from the four quadrants of the $[-3,3] \times [-3,3]$ grid. We then define a transformation $\boldsymbol{z}' = (z'_1, \ldots, z'_{100})$ of $\boldsymbol{z}$ through one of the following functions:

1. (scaling)
$$z'_i = 5z_i;$$
2. (translation)
$$z'_i = (z_i + 5);$$
3. (translation in opposite directions)
$$z'_i = (z_i \pm 5)$$
(+ for $1 \leq i \leq 50$ and − for $51 \leq i \leq 100$), which translates two halves of the map in opposite directions.

We add independent Gaussian noises $N(0, 0.1^2)$ to $\boldsymbol{z}$ and $\boldsymbol{z}'$ at the $(x_i, y_i), i = 1, \ldots, 100$, to create two groups of power maps $\{\boldsymbol{z}_1, \ldots, \boldsymbol{z}_5 : \boldsymbol{z}_j = (z_{j1}, \ldots, z_{j100})\}$ and $\{\boldsymbol{z}'_1, \ldots, \boldsymbol{z}'_5 : \boldsymbol{z}'_j = (z'_{j1}, \ldots, z'_{j100})\}$.

Under each transformation setting, this simulation procedure is repeated 500 times; for each simulation, the null hypothesis (4) is tested on the 2 groups of 5 samples through the proposed permutation test with 252 exact permutations. We reject the null when a p-value falls below 0.05. The rejection rates are 5%, 3% and 98% in each setting. The results provide numerical evidence that the proposed procedure for testing the difference between topographic maps stays robust under some scaling and translation and meanwhile is sensitive to translation in opposite directions. In comparison, the maximum t-statistic test has rejection rates of 9%, 6% and 99% in each setting. It is more sensitive than the proposed topological inference procedure in picking up non-topological difference between power maps.

4 Real Data Application

Data description. The aim of this application is to compare topological difference between frequency variations in the EEG signals of 24 meditation-naïve participatns (MNPs) and 24 long-term meditators (LTMs) of Buddhist meditation practices (approximately 8700 mean hours of life practice) during whole-night non-rapid eye movement (NREM) sleep divided into 3 cycles. The EEG

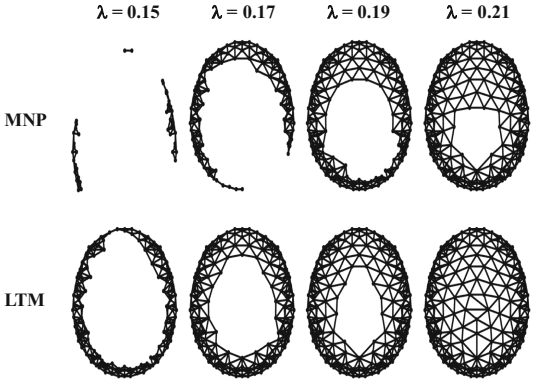

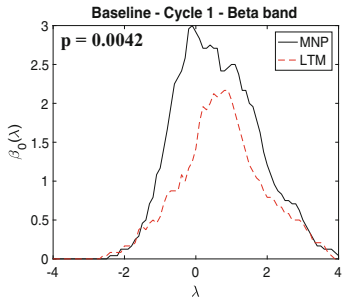

Baseline	Method	Cycle 1	Cycle 2	Cycle 3
β	β_0 test	0.0042	0.0274	0.0430
[15, 25]Hz	max-t test	0.0072	0.0062	0.0032
γ	β_0 test	0.6988	0.5094	0.1426
[25, 40]Hz	max-t test	0.0342	0.0004	0.0114

Fig. 2. Left: Filtrations of mean normalized power maps in the beta band in sleep cycle 1 under the baseline condition. Right top: Group mean β_0 functions with the p-value from the β_0 permutation test. Right bottom: The p-values of β_0 and maximum t-statistic permutation tests comparing MNPs and LTMs in the baseline session. The p-values below the Bonferonni threshold $0.05/6 = 0.0083$ corrected over 2 (frequency bands) $\times$ 3 (sleep cycles) $= 6$ tests for each method are shaded in gray.

signals were recorded with a 256-channel hdEEG system (Electrical Geodesics Inc., Eugene, OR). Signals bandpass filtered (1–50 Hz), and independent component analysis was used to remove ocular and muscle artifacts in the signals. More pre-processing details can be found in [3]. The participants undergo 3 sessions of recording: a baseline session, and one session each after two days of Vipassana (mindfulness) and Metta (compassion) meditations. We analyze the baseline session for unconfounded effect of long-term meditation practice. Also, we focus on the high-frequency bands β and γ of the EEGs since high frequency has been shown to positively correlate with meditation experience [6].

Topological permutation test. After heat kernel denoising with a moderate bandwidth $\sigma = 0.5$ for the noise level in the data, we normalize each power map by a z-score transformation across all channels. We then compare the normalized denoised power maps of the LTMs and MNPs in the high-frequency β (15–25 Hz) and γ (25–40 Hz) bands by the proposed permutation test. For β band in sleep cycle 1, the node-based network filtrations of the average normalized maps in both groups are shown in Fig. 2 (left). The closure of clusters is distinctly faster in the average LTM map as λ increases. Figure 2 (right top) shows the average β_0 functions of LTMs and MNPs in the β band of sleep cycle 1. The LTM function is below the MNP function throughout the range of λ values, meaning that on average the LTMs have fewer clusters than the MNPs. This implies that the LTM power maps having more coherent spatial distribution, as nodes with similar powers get connected in a smaller window of λ than those with more varied powers.

Comparison with maximum t-statistic test. The table of p-values in Fig. 2 provides comparison between results of the proposed and maximum t-statistic permutation test. The only place where the proposed test shows significant topological difference is the β band in sleep cycle 1, whereas the maximum t-statistic test shows significant difference between LTM and MNP in four out of six categories. Due to sensitivity shown by the maximum t-statistic approach in simulations, it is possible that we are getting signals from non-topological difference between the two groups of power maps.

5 Discussion

In this paper, the spatial distribution of an EEG topographic power map is quantified through a novel node-based network filtration. We use the network filtration to compare the spatial distribution of EEG power maps in long-term meditators and meditation naïve practitioners. The results show that the meditators have on average fewer clusters, thus a more coherent spatial distribution, than novices in the early stage of NREM sleep.

In EEG analysis, a general concern is that the scalp signal at each electrode is a weighted sum of the signal generated by all cortical sources. For future research, we will also explore an unmixing procedure such as working in source space after applying a distributed solution and analyzing selected independent components. It will provide deeper insight into the underlying neurophysiological dynamics that the topological network analysis has the potential to capture.

Acknowledgment. This work was supported by the National Center for Complementary and Alternative Medicine (NCCAM) P01AT004952. We also acknowledge the support of NIH grants UL1TR000427 and EB022856.

References

1. Brunet, D., Murray, M.M., Michel, C.M.: Spatiotemporal analysis of multichannel EEG: CARTOOL. Comput. Intell. Neurosci. **2011**, 15 (2011)
2. Davidson, R.J., Lutz, A.: Buddha's brain: neuroplasticity and meditation. IEEE Signal Process. Mag. **25**(1), 176–174 (2008)
3. Dentico, D., Ferrarelli, F., Riedner, B.A., Smith, R., Zennig, C., Lutz, A., Tononi, G., Davidson, R.J.: Short meditation trainings enhance non-REM sleep low-frequency oscillations. PLoS ONE **11**(2), e0148961 (2016)
4. Edelsbrunner, H., Harer, J.: Computational Topology. American Mathematical Society, Providence (2010)
5. Eklund, A., Nichols, T.E.T.E., Knutsson, H.: Cluster failure: why fMRI inferences for spatial extent have inflated false-positive rates. Proc. Nat. Acad. Sci. **113**(33), 7900–7905 (2016)
6. Ferrarelli, F., Smith, R., Dentico, D., Riedner, B.A., Zennig, C., Benca, R.M., Lutz, A., Davidson, R.J., Tononi, G.: Experienced mindfulness meditators exhibit higher parietal-occipital EEG gamma activity during NREM sleep. PLoS ONE **8**(8), e73417 (2013)

7. Maris, E.: Statistical testing in electrophysiological studies. Psychophysiology **49**(4), 549–565 (2012)
8. Maris, E., Oostenveld, R.: Nonparametric tatistical testing of EEG- and MEG-data. J. Neurosci. Methods **164**(1), 177–90 (2007)
9. Mensen, A., Khatami, R.: Advanced EEG analysis using threshold-free cluster-enhancement and non-parametric statistics. NeuroImage **67**, 111–118 (2013)
10. Welch, P.: The use of fast Fourier transform for the estimation of power spectra: A method based on time averaging over short, modified periodograms. IEEE Trans. Audio Electroacoust. **15**(2), 70–73 (1967)